

NASA Technical Memorandum 102338

Refinements in a Viscoplastic Model

A.D. Freed
Lewis Research Center
Cleveland, Ohio

and

K.P. Walker
Engineering Science Software
Smithfield, Rhode Island

Prepared for the
1989 Winter Annual Meeting
of the American Society of Mechanical Engineers
San Francisco, California, December 10-15, 1989



(NASA-TM-102338) REFINEMENTS IN A
VISCOPLASTIC MODEL (NASA. Lewis Research
Center) 18 p CSCL 20K

N89-28036

Unclas
0225965

G3/39

REFINEMENTS IN A VISCOPLASTIC MODEL

A. D. Freed

National Aeronautics and Space Administration
Lewis Research Center
Cleveland, OH 44135

K. P. Walker

Engineering Science Software, Inc.
Smithfield, RI 02917

ABSTRACT

A thermodynamically admissible theory of viscoplasticity with two internal variables (a back stress and a drag strength) is presented. Six material functions characterize a specific viscoplastic model. In the pursuit of compromise between accuracy and simplicity, a model is developed that is a hybrid of two existing viscoplastic models. A limited number of applications of the model to Al, Cu, and Ni are presented. A novel implicit integration method is also discussed, and applications are made to obtain solutions using this viscoplastic model.

NOMENCLATURE

material constants

$a, A, A', b, c, D_0, E, h, H_1, H_2, k, m, n, n', Q, T_i, \alpha, \nu$

magnitudes

$|B|, |S|, |S-B|, |S-X|, |X|, |\dot{\epsilon}^p|, \dot{W}^v$

internal variables

$B_{ij}, D, X_{ij}, \beta_{ij}^1, \beta_{ij}^2, \delta$

direction tensors

$d_{ij}, n_{ij}, u_{ij}, x_{ij}$

material functions

$l, L, r, R, Z, Z_{ss}, \theta$

strains and stresses

$e_{ij}, S_{ij}, \epsilon_{ij}, \epsilon_{ij}^e, \epsilon_{ij}^p, \sigma_{ij}$

1. INTRODUCTION

The design of structures exposed to high-temperature environments requires mathematical models capable of accurately predicting short-term plastic strains, long-term creep strains, and the interactions between them. Multiaxial, cyclic, and nonisothermal loading histories are normal service conditions, not exceptional ones. In the pursuit to achieve this objective, a hybrid model is developed using WALKER's [1] theoretical structure for the evolution of internal state and MILLER's [1] methodology for characterizing material functions. The main reason for doing inelastic analysis is not so much to determine the deformation response of the structure *per se*, but rather to assess its useful service life. Results from inelastic analysis are input to life assessing schemes. These

schemes typically require such quantities as: stress range, mean stress, inelastic strain range, and the percentages of time-dependent creep and time-independent plasticity that make up the inelastic strain range [3]. It is therefore important that the mathematical model used in high-temperature structural analysis be capable of predicting these parameters with reasonable accuracy.

A wide range of materials are used in structures that are designed to operate in high-temperature environments. The designer's choice of material is usually dictated by cost and by such factors as its ability to: carry load, conduct heat, resist crack initiation and growth, and resist oxidation and corrosion. A typical metal may have some desirable properties, and some undesirable ones as well. With the technology of metal-matrix fabrication coming of age, the engineer can now begin to tailor materials that provide optimal characteristics for a given application. At NASA, composite matrices of aluminum, copper, nickel, and their alloys are being considered for a variety of applications. Along with ceramics, tungsten and tungsten alloys are being considered as fiber materials. An objective of this paper is to develop a model for characterizing their viscoplastic behavior. These material representations will be used in the near future in a mesomechanics model [4,5] to predict the viscoplastic response of metal matrix composites.

The need for reliable and expedient algorithms to numerically integrate viscoplastic models is of paramount importance. Such models are composed of systems of stiff, first-order, linear, differential equations whose coefficients are coupled and strongly nonlinear; hence, they are inherently difficult to integrate. The implicit integration algorithm of WALKER [6,7], which is presented in appendix A and extended there to include the second-order term in its difference formulation, is applied to our viscoplastic model.

2. VISCOPLASTIC THEORY

The structure of our viscoplastic theory is a special case of a much more general structure that FREED & CHABOCHE [8] have shown to be physically motivated and thermodynamically admissible. The theory admits two fundamental internal variables; they are: the (positive scalar-valued) drag strength $D > 0$, and the (deviatoric tensor-valued) back stress B_{ij} . The drag strength accounts for isotropic hardening effects. The back stress accounts for kinematic (or flow-induced anisotropic) hardening effects, and is considered to be the sum of two separately evolving constituents. One constituent B_{ij}^1 represents short-range back stress effects, while the other constituent B_{ij}^2 represents long-range back stress effects [9,10]. These internal variables are considered to evolve phenomenologically through competitive processes associated with strain hardening, strain-induced dynamic recovery, and time-induced thermal recovery.

The strain ϵ_{ij} is taken to be the sum of an elastic (or thermodynamically reversible) strain ϵ_{ij}^e and an inelastic (or thermodynamically irreversible) strain ϵ_{ij}^p , i.e.,

$$\epsilon_{ij} = \epsilon_{ij}^e + \epsilon_{ij}^p \quad (1)$$

with no inelastic strain occurring in the stress-free virgin state. Small strains, displacements, and rotations are considered to make up the deformation of a material element.

The *constitutive equations* of the theory are given by:

$$\epsilon_{ij}^e = \frac{1+\nu}{E} \sigma_{ij} - \frac{\nu}{E} \sigma_{kk} \delta_{ij} + \alpha(T-T_0)\delta_{ij} \quad (2a)$$

$$B_{ij} = \sum_{\gamma=1}^2 B_{ij}^{\gamma} = \frac{2}{3} \sum_{\gamma=1}^2 H_{\gamma} \beta_{ij}^{\gamma} \quad (2b)$$

$$D = D_0 + h \delta \quad (2c)$$

where E is the elastic modulus, ν is the Poisson ratio, α is the coefficient of thermal expansion, $T-T_0$ is the change in temperature, σ_{ij} is the stress, and δ_{ij} is the Kronecker delta. Here β_{ij}^{γ} and $\delta \geq 0$ are the thermodynamic displacements conjugate to the thermodynamic forces B_{ij}^{γ} and $D-D_0 \geq 0$, with $H_{\gamma} > 0$ and $h > 0$ denoting their hardening coefficients, and $D_0 > 0$ defining the annealed value of drag strength. Repeated Latin indices are summed over from 1 to 3 in the usual manner.

The *evolution equations* of the theory are given by:

$$\dot{\epsilon}_{ij}^p = \theta Z n_{ij} = |\dot{\epsilon}^p| n_{ij} \quad (3a)$$

$$\dot{\beta}_{ij}^1 = \dot{\epsilon}_{ij}^p - \frac{|X|}{L} |\dot{\epsilon}^p| d_{ij} - \theta R x_{ij} \quad (3b)$$

$$\dot{\beta}_{ij}^2 = \dot{\epsilon}_{ij}^p \quad (3c)$$

$$\dot{\delta} = \left[\frac{1}{D-D_0} - \frac{1}{l} \right] \dot{W}^v - \theta r \quad (3d)$$

which, when combined with the constitutive equations (2b and 2c), give rise to the governing viscoplastic equations of our theory; they are:

$$\dot{\epsilon}_{ij}^p = \theta Z n_{ij} = |\dot{\epsilon}^p| n_{ij} \quad (4a)$$

$$\begin{aligned} \dot{B}_{ij} = & \frac{2}{3}(H_1+H_2) \dot{\epsilon}_{ij}^p - \frac{2}{3}H_1 \left[\frac{|X|}{L} |\dot{\epsilon}^p| d_{ij} + \theta R x_{ij} \right] + \\ & + \frac{\dot{H}_1}{H_1} B_{ij} + \frac{2}{3} \left[\dot{H}_2 - \frac{H_2}{H_1} \dot{H}_1 \right] \epsilon_{ij}^p \end{aligned} \quad (4b)$$

$$\dot{D} = h \left[\left[\frac{1}{D-D_0} - \frac{1}{l} \right] \dot{W}^v - \theta r \right] + \frac{D-D_0}{h} \dot{h} \quad (4c)$$

where

$$X_{ij} = B_{ij} - \frac{2}{3} H_2 \epsilon_{ij}^p \equiv B_{ij}^1 \quad (5a)$$

$$\dot{W}^v = (S_{ij} - B_{ij}) \dot{\epsilon}_{ij}^p = |S-B| |\dot{\epsilon}^p| \quad (5b)$$

with directions (unit or projection) defined by:

$$n_{ij} = \frac{3}{2} \frac{S_{ij}-B_{ij}}{|S-B|}, \quad u_{ij} = \frac{3}{2} \frac{S_{ij}-X_{ij}}{|S-X|}, \quad x_{ij} = \frac{3}{2} \frac{X_{ij}}{|X|} \quad (5c)$$

$$d_{ij} = (1-a) x_{ij} + a \frac{u_{kl} X_{kl}}{|X|} u_{ij} \quad (5d)$$

and with norms (or magnitudes) defined by:

$$|\dot{\epsilon}^p| = \sqrt{(2/3) \dot{\epsilon}_{ij}^p \dot{\epsilon}_{ij}^p}, \quad |J| = \sqrt{(3/2) J_{ij} J_{ij}} \quad (5e)$$

where $J_{ij} \in \{S_{ij}, B_{ij}, S_{ij}-B_{ij}, X_{ij}, S_{ij}-X_{ij}\}$, $S_{ij} = \sigma_{ij} - \sigma_{kk} \delta_{ij}/3$ is the deviatoric stress, and $S_{ij}-B_{ij}$ is the viscous stress that drives inelastic flow. This choice for the directions and norms scales the theory for tension. The notation $X_{ij} \equiv B_{ij}^1$ is used for easier visual distinction between X_{ij} and B_{ij} . The derivatives of the hardening coefficients \dot{h} , \dot{H}_1 and \dot{H}_2 represent their change with temperature, if any.

The material functions of the theory are: $\theta(T) > 0$ is the thermal diffusivity, $Z(|S-B|/D) = |\dot{\epsilon}^p|/\theta \geq 0$ is the Zener [11] parameter, $L > 0$ and $l > 0$ are the limiting states associated with dynamic recovery, and $R \geq 0$ and $r \geq 0$ are the thermal recovery functions. At this point in the development, the limit and thermal-recovery functions are general functions of state. Specific forms for the functions θ , Z , l , L , r , and R will vary from model to model. There is one material constant in these evolution equations; it is the nonproportionality parameter $a \in [0,1]$ found in eqn. (5d). This parameter provides added flexibility in modeling nonproportional kinematic behavior; it has no effect on proportional behavior. What it does (more or less) is proportion the nonlinear strain-induced characteristics of the back stress between the mechanisms of hardening and recovery [8]. The value of this parameter has a profound impact on predicted response under nonproportional ratchetting conditions [12].

Notice that the drag strength D evolves with $\dot{W}^v/(D-D_0)$. It cannot evolve with either $|\dot{\epsilon}^p|$ or $S_{ij} \dot{\epsilon}_{ij}^p$ (the choices in existing models), and satisfy the thermodynamic constraint of intrinsic dissipation throughout the entire domain of state space [8] defined by the set $\{T, \sigma_{ij}, D, B_{ij}\}$. Therefore, in the absence of recovery, the drag strength parabolically hardens with viscous work, i.e., $D \propto \sqrt{W^v}$. Parabolic hardening of the drag strength was introduced phenomenologically by MILLER & SHERBY [13] into their model; here it is introduced as a direct consequence of the thermodynamics. Because $D-D_0$ is in the denominator of this forcing function, it appears to be singular in the virgin state, $D = D_0$. But actually the forcing function is zero valued there, because the numerator, \dot{W}^v , is zero valued in the virgin state, too.

The basic form of the evolution equations (3b and 3c) for the kinematic variables β_{ij}^1 and β_{ij}^2 was proposed by WALKER [1], and is a compromise between accuracy and simplicity. By assuming that the long-range back stress B_{ij}^2 does not thermally recover, which is physically incorrect (a compromise), it can be integrated exactly and combined with the short-range back stress $B_{ij}^1 \equiv X_{ij}$. The result is a single governing equation (4b) for the back stress (instead of two) which has both short- and long-range features providing improved accuracy. The direction for dynamic recovery d_{ij} of the back stress, as established in eqn. (5d), presents a refinement to the original theory. Dynamic recovery is taken to be proportioned by a factor a between directions opposing the short-range back stress X_{ij} and the stress difference $S_{ij}-X_{ij}$. The scaling factor $u_{ij}X_{ij}/|X|$ in eqn. (5d) is introduced to make the model insensitive to the direction of dynamic recovery under proportional loading conditions (*i.e.*, the predicted response is the same for all values of the parameter $a \in [0,1]$). The model only becomes sensitive to the direction of dynamic recovery (*i.e.*, the value of a) under nonproportional loading conditions. This scaling factor is also required for the theory to be thermodynamically admissible [8].

3. VISCOPLASTIC MODEL

Our model is predicated upon the assumption that the magnitude of inelastic strain rate (in particular, Z_{ss}) can be represented as a sum of two power functions in stress (*cf.* appendix B). One to govern at the higher-temperatures/lower-stresses, while the other to govern at the lower-temperatures/higher-stresses. An analogous expression for Z has recently been proposed by CHABOCHE [14] to model the transient strain-rate sensitivity of a stainless steel. This parameter is a generalization of WALKER's [1] power-law model, and a simplification (especially from a numerical integration viewpoint) of MILLER's [2] hyperbolic sine model, *i.e.*, a compromise between accuracy and simplicity. We motivate its choice with the steady-state creep data of fig. 1, where $Z_{ss} = |\dot{\epsilon}^c|/\theta$. By applying Miller's hypothesis (*cf.* appendix B) to our relationship for the stress dependence of inelastic flow at steady state, we are able to obtain explicit relationships for the transient Zener parameter Z , and both of the thermal recovery functions r and R . Details on the derivation of the material functions, and a procedure for determining values for their associated constants, are presented in appendix B.

The *material functions* of our viscoplastic model are:

$$\theta = \begin{cases} \exp\left\{\frac{-Q}{kT}\right\} & ; \frac{T}{T_i} \geq 1 \\ \exp\left\{\frac{-Q}{kT_i}\left[\ln\left(\frac{T_i}{T}\right) + 1\right]\right\} & ; \frac{T}{T_i} \leq 1 \end{cases} \quad (6a)$$

$$Z = \left[\frac{|S-B|}{D}\right]^{mn} + \left[\frac{A}{A'}\right]^{n'} \left[\frac{|S-B|}{D}\right]^{mn'} \quad (6b)$$

$$L = c D \quad (6c)$$

$$R = \left[\frac{H_1+H_2}{H_1} - \frac{|X|}{L}\right] \left[\left[\frac{|B|}{bA}\right]^n + \left[\frac{|B|}{bA'}\right]^{n'}\right] \quad (6d)$$

$$l = \infty \quad (6e)$$

$$r = \frac{D}{D-D_0} H(D-D_0) \left[\left[\frac{D}{A(1-b)}\right]^{\frac{1+mn}{m-1}} + \left[\frac{A}{A'}\right]^{n'} \left[\frac{D}{A(1-b)}\right]^{\frac{1+mn'}{m-1}} \right] \quad (6f)$$

where eqn. (6e) implies no dynamic recovery of the drag strength. (A particular limit function l is under consideration to account for monotonic/cyclic interactions, which are not incorporated in the current model, *i.e.*, $l = \infty$.) The *material constants* for this model are comprised of: the elastic constants: E , α , and ν ; the thermal activation energy and transition temperature: Q and T_i ; the steady-state constants: A , A' , n , and n' ; the constant-structure constant: m ; the threshold constants: b and c ; the transient constants: h , H_1 , and H_2 ; the nonproportional constant: a ; and the initial values: D_0 and $D(t=0)$. The parameter k is the Boltzmann constant, and $H(D-D_0)$ is the Heaviside function. Values for these constants are given in table 1 for aluminum, copper, nickel, and tungsten. If one chooses, a reference temperature could be introduced (thereby setting $\theta(T_{ref})=1$) which would, in effect, scale the drag strength.

This model has several deficiencies that the authors are aware of, and are working on. It does not account for monotonic/cyclic interaction effects. It overpredicts normal ratcheting behavior. And it does not account for inverse strain rate sensitivity effects exhibited by many alloys. These deficiencies are common amongst most viscoplastic models found in the literature.

4. NUMERIC INTEGRATION

One can combine the constitutive equations (2) and the evolution equations (3) of our viscoplastic theory and obtain the following system of stiff, linear, first-order, difference equations:

$$\Delta \Sigma_{ij} + \Sigma_{ij} \Delta a = \Delta x_{ij} \quad (7a)$$

$$\Delta X_{ij} + X_{ij} \Delta b = \Delta y_{ij} \quad (7b)$$

$$\Delta K + K \Delta c = \Delta z \quad (7c)$$

with

$$S_{ij} = \Sigma_{ij} + B_{ij} \quad (8a)$$

$$B_{ij} = X_{ij} + \frac{2}{3} H_2 \epsilon_{ij}^p \quad (8b)$$

$$\epsilon_{ij}^p = e_{ij} - \frac{S_{ij}}{2\mu} \quad (8c)$$

$$D = D_0 + \sqrt{2K} \quad (8d)$$

where the coefficients are nonlinear and coupled, and are defined by:

$$\Delta a = \frac{3\mu}{|S-B|} |\Delta \epsilon^p| - \frac{1}{\mu} \Delta \mu \quad (9a)$$

$$\Delta b = H_1 \left[\frac{1-a}{L} |\Delta \epsilon^p| + \theta \frac{R}{|X|} \Delta t \right] - \frac{1}{H_1} \Delta H_1 \quad (9b)$$

$$\Delta c = 2 \left[h \left[\frac{1}{l} \frac{|S-B|}{D-D_0} |\Delta \epsilon^p| + \theta \frac{r}{D-D_0} \Delta t \right] - \frac{1}{h} \Delta h \right] \quad (9c)$$

and where the nonhomogeneous terms are also nonlinear and coupled, and are defined by:

$$\Delta x_{ij} = 2\mu \Delta e_{ij} - \Delta B_{ij} + \frac{B_{ij}}{\mu} \Delta \mu \quad (10a)$$

$$\Delta y_{ij} = \frac{2}{3} H_1 \left[n_{ij} - a \frac{u_{kl} X_{kl}}{L} u_{ij} \right] |\Delta \epsilon^p| \quad (10b)$$

$$\Delta z = h |S-B| |\Delta \epsilon^p| \quad (10c)$$

Here $\Delta \mu$, Δh , and ΔH_1 represent the incremental change in these moduli due to an incremental change ΔT in temperature. This system of difference equations characterizes the deviatoric response of the material, while the constitutive equation $\sigma_{ii} = 3\kappa[\epsilon_{ii} - \alpha(T-T_0)\delta_{ii}]$ characterizes the hydrostatic response of the material. Here $\mu = E/2(1+\nu)$ is the elastic shear modulus, and $\kappa = E/3(1-2\nu)$ is the elastic bulk modulus.

The system of difference equations (7) can be solved by classical methods, such as the explicit methods of Euler and Runge-Kutta. Such methods require numerous time steps in order to maintain numeric stability and accuracy because the coefficients and nonhomogeneous terms make this system of equations mathematically stiff. This is not a detriment when numerous data pairs are needed to plot smooth accurate response curves. However a new method, the uniformly-valid implicit integration scheme of WALKER [6], may be preferred for finite element analyses where computational times are large, and the ability to create smooth response curves at the nodal points is not the typical required output [7]. An advantage of this method is that it is not constrained by time step size in order to maintain numeric stability and accuracy since the scheme is uniformly valid. Walker's method transforms the system of difference equations (7) into recursive integral equations, which are then solved using an asymptotic expansion technique (*cf.* appendix A). The resulting integration scheme for the

general viscoplastic theory presented in eqn. (4) is given by the following system of stiff, coupled, implicit, recursive relations:

$$\begin{aligned} \Sigma_{ij}(t+\Delta t) = & \Sigma_{ij}(t) e^{-\Delta a(t+\Delta t)} + \frac{\Delta x_{ij}(t+\Delta t)}{\Delta a(t+\Delta t)} \left[1 - e^{-\Delta a(t+\Delta t)} \right] + \\ & + \frac{\Delta x_{ij}(t+\Delta t) - \Delta x_{ij}(t)}{\Delta a(t+\Delta t)} \left[e^{-\Delta a(t+\Delta t)} - \frac{1}{\Delta a(t+\Delta t)} \left[1 - e^{-\Delta a(t+\Delta t)} \right] \right] \end{aligned} \quad (11a)$$

$$\begin{aligned} X_{ij}(t+\Delta t) = & X_{ij}(t) e^{-\Delta b(t+\Delta t)} + \frac{\Delta y_{ij}(t+\Delta t)}{\Delta b(t+\Delta t)} \left[1 - e^{-\Delta b(t+\Delta t)} \right] + \\ & + \frac{\Delta y_{ij}(t+\Delta t) - \Delta y_{ij}(t)}{\Delta b(t+\Delta t)} \left[e^{-\Delta b(t+\Delta t)} - \frac{1}{\Delta b(t+\Delta t)} \left[1 - e^{-\Delta b(t+\Delta t)} \right] \right] \end{aligned} \quad (11b)$$

$$\begin{aligned} K(t+\Delta t) = & K(t) e^{-\Delta c(t+\Delta t)} + \frac{\Delta z(t+\Delta t)}{\Delta c(t+\Delta t)} \left[1 - e^{-\Delta c(t+\Delta t)} \right] + \\ & + \frac{\Delta z(t+\Delta t) - \Delta z(t)}{\Delta c(t+\Delta t)} \left[e^{-\Delta c(t+\Delta t)} - \frac{1}{\Delta c(t+\Delta t)} \left[1 - e^{-\Delta c(t+\Delta t)} \right] \right] \end{aligned} \quad (11c)$$

where $t \geq 0$ and where $\Delta t > 0$ may be arbitrarily large or small. These equations must be solved simultaneously using a technique such as Newton-Raphson iteration, where Δa , Δb , and Δc are the iterated variables [6,7]. For viscoplastic models that have a back stress and a drag strength (or yield strength) which evolve, Walker's implicit integration scheme has only three variables to iterate over; whereas, the classical implicit integration schemes (*e.g.* backward Euler difference) have thirteen variables to iterate over (*i.e.*, six for inelastic strain, six for back stress, and one for drag strength).

5. APPLICATIONS

A few applications for aluminum, copper, and nickel (data are insufficient to include tungsten) are presented to demonstrate some of the capabilities and limitations of the model, and to show feasibility of the Walker integration method.

The model's capability in predicting the monotonic behavior of aluminum as a function of temperature is demonstrated in fig. 2. The model produces acceptable predictions above approximately $.2 T_h$ (or about -100°C , where T_h is the material's homologous temperature). This is an improvement over a single power-law for the Zener parameter with an exponent of $n \approx 5$, which produces acceptable predictions above approximately $.5 T_h$ (or about 200°C for aluminum). In applications requiring modeling at both elevated temperatures and temperatures below $.2 T_h$, the hyperbolic Zener parameter of MILLER [2] is recommended. Numeric integration using the technique of Walker described in the previous section and the second-order method of Runge-Kutta with automatic time-step control was done here with good agreement between the two methods (less than 1 MPa difference, with a maximum error of 20% which occurred at the highest temperatures where the stress is on the order of 5 MPa in fig. 2). The method of Walker was found to be superior to that of Runge-Kutta in both accuracy and computation time. This was especially true when the model became mathematically stiff (*i.e.*, in the regions where hardening and recovery mechanisms are of comparable magnitude). Here the difference in *cpu* times exceeded an order in magnitude, and the Runge-Kutta solutions oscillated.

A thermomechanical prediction of the model (in this case, for nickel) is presented in fig. 3a. The model produces the correct shape of the hysteresis loop with two exceptions. Of course, it cannot model the serrated yielding (or strain avalanching, [28]) observed in the experimental response. And second, the model presently has no provision to account for monotonic/cyclic interactions, and therefore it continues to isotropically harden beyond that which is experimentally observed. This deficiency is being worked on.

Figure 3b presents a comparison between predictions obtained using the methods of Walker (with several different time steps) and second-order Runge-Kutta (with automatic time stepping). The Walker analysis with the largest time step size ($50^\circ\text{C} / \text{step}$) ran about 2.5 times faster than the Runge-Kutta analysis, the one with the intermediate time step (approximately $15^\circ\text{C} / \text{step}$) ran about 1.5 times faster, while the one with the smallest time step ($1.5^\circ\text{C} / \text{step}$) ran about 3 times slower. The greatest variation in the three Walker solutions occurs at the knees of the hysteresis curve. A benefit of the Walker (implicit integral) method is that this error is not

propagated, as all three solutions agree at the turnaround points. This is not true of explicit differential methods, such as Runge-Kutta, where an error initiated is also propagated. The effect of a slowly accumulated propagating error is found in the Runge-Kutta solution, and can be observed by looking at successive peaks in fig. 3b.

The model's capability in predicting nonproportional material behavior (for copper) is demonstrated in fig. 4. Here the influence of the nonproportionality parameter a on predicted response is shown. The limiting case of $a = 0$ represents the nonlinear kinematic hardening rule of Armstrong and Frederick [9,14], while the other extreme of $a = 1$ denotes a nonlinear Prager-like hardening rule [8,12]. The prediction for $a = 1$ produces an unwanted ratchetting down the axial stress axis; a result also observed by LAMBA & SIDEBOTTOM [29] in plasticity analyses using the Prager and Ziegler hardening rules. There is little difference in the predicted response over a wide range in the parameter a ($a = 0$ to $a \approx 0.9$ in this experiment). Therefore a more severe nonproportional loading history (such as advocated in ref. 12) is necessary to characterize the value of the material constant a . This figure illustrates another limitation of the model. Our model, like most, is formulated with a von Mises type norm, whereas copper behaves like a Tresca material [29]. That is why the predicted axial stress response is too soft, as the value of the drag strength was correlated with the shear response in this figure.

6. CONCLUSIONS

Within the framework of a thermodynamically admissible theory of viscoplasticity with an evolving back stress and drag strength, a model is presented that is a hybrid of the WALKER [1] and MILLER [2] models. The model is for pure metals, and has been applied to aluminum, copper, and nickel. Tungsten has been partially characterized, using rules of thumb instead of experimental data (they do not exist) to establish values for roughly half of the constants. Both strengths and weaknesses of the model are discussed. The implicit integration scheme of WALKER [6,7] has been further developed and applied to our model, and was found to be superior to the second-order method of Runge-Kutta. A detailed numerical study of the Walker integration technique is currently underway.

REFERENCES

- [1] Walker, K. P., 1981, "Research and Development Program for Nonlinear Structural Modeling With Advanced Time-Temperature Dependent Constitutive Relationships," *NASA CR-165533*.
- [2] Miller, A., 1976, "An Inelastic Constitutive Model for Monotonic, Cyclic, and Creep Deformation: Part I - Equations Development and Analytical Procedures," *J. Eng. Mater. Technol.*, Vol. 96, p. 97.
- [3] Saltsman, J. F., and Halford, G. R., 1988, "Life Prediction of Thermomechanical Fatigue Using Total Strain Version of Strainrange Partitioning (SRP): A Proposal," *NASA TP-2779*.
- [4] Walker, K. P., Jordan, E. H., and Freed, A. D., 1989, "Nonlinear Mesomechanics of Composites With Periodic Microstructure: First Report," *NASA TM-102051*.
- [5] Walker, K. P., Jordan, E. H., and Freed, A. D., 1989, "Equivalence of Green's Function and the Fourier Series Representation of Composites With Periodic Microstructure," *Micromechanics and Inhomogeneity - The Toshio Mura Anniversary Volume*, Springer-Verlag, p. 535.
- [6] Walker, K. P., 1987, "A Uniformly Valid Asymptotic Integration Algorithm for Unified Viscoplastic Constitutive Models," *Advances in Inelastic Analysis*, S. Nakazawa *et al.*, eds., AMD - Vol. 88 / PED - Vol. 28, ASME, p. 13.
- [7] Chulya, A., and Walker, K. P., 1989, "A New Uniformly Valid Asymptotic Integration Algorithm for Elasto-Plastic-Creep and Unified Viscoplastic Theories Including Continuum Damage," to appear: *NASA TM*.
- [8] Freed, A. D., and Chaboche, J. L., "Viscoplasticity: A Thermodynamic Formulation," submitted to: *J. Appl. Mech.*
- [9] Chaboche, J. L., and Rousselier, G., 1983, "On the Plastic and Viscoplastic Constitutive Equations - Part I: Rules Developed With Internal Variable Concept," *J. Pressure Vessel Technol.*, Vol. 105, p. 153.
- [10] Lowe, T. C., and Miller, A. K., 1986, "Modeling Internal Stresses in the Nonelastic Deformation of Metals," *J. Eng. Mater. Technol.*, Vol. 108, p. 365.

- [11] Zener, C., and Hollomon, J. H., 1944, "Effect of Strain Rate Upon Plastic Flow of Steel," *J. Appl. Phys.*, Vol. 15, p. 22.
- [12] Burlet, H., and Cailletaud, G., 1987, "Modeling of Cyclic Plasticity in Finite Element Codes," *Constitutive Laws for Engineering Materials: Theory and Applications*, C. S. Desai *et al.*, eds., Elsevier Applied Science, New York, p. 1157.
- [13] Miller, A. K., and Sherby, O. D., 1978, "A Simplified Phenomenological Model for Non-Elastic Deformation: Predictions of Pure Aluminum Behavior and Incorporation of Solute Strengthening Effects," *Acta Metall.* Vol. 26, p. 289.
- [14] Chaboche, J. L., 1989, "Constitutive Equations for Cyclic Plasticity and Cyclic Viscoplasticity," to appear: *Int. J. Plast.*.
- [15] Weertman, J., 1956, "Creep of Polycrystalline Aluminum as Determined from Strain Rate Tests," *J. Mech. Phys. Solids*, Vol. 4, p. 230.
- [16] Servi, I. S., and Grant, N. J., 1951, "Creep and Stress Rupture Behavior of Aluminum as a Function of Purity," *J. Metals*, Vol. 3, p. 909.
- [17] Luthy, H., Miller, A. K., and Sherby, O. D., 1980, "The Stress and Temperature Dependence of Steady-State Flow at Intermediate Temperatures for Pure Polycrystalline Aluminum," *Acta Metall.*, Vol. 28, p. 169.
- [18] Jenkins, W. D., and Digges, T. G., 1951, "Creep of Annealed and Cold-Drawn High-Purity Copper," *J. Res. NBS*, Vol. 47, p. 272.
- [19] Barrett, C. R., and Sherby, O. D., 1964, "Steady-State Creep Characteristics of Polycrystalline Copper in the Temperature Range 400° to 950°C," *Trans. AIME*, Vol. 230, p. 1322.
- [20] Pahutová, M., Čadek, J., and Ryš, P., 1971, "High Temperature Creep in Copper," *Philos. Mag.*, Vol. 23, p. 509.
- [21] Jenkins, W. D., Digges, T. G., and Johnson, C. R., 1954, "Creep of High-Purity Nickel," *J. Res. NBS*, Vol. 53, p. 329.
- [22] Weertman, J., and Shahinian, P., 1956, "Creep of Polycrystalline Nickel," *J. Metals*, Vol. 8, p. 1223.
- [23] King, G. W., and Sell, H. G., 1965, "The Effect of Thoria on the Elevated-Temperature Tensile Properties of Recrystallized High-Purity Tungsten," *Trans. AIME*, Vol. 233, p. 1104.
- [24] Klopp, W. D., Witzke, W. R., and Raffo, P. L., 1965, "Effect of Grain Size on Tensile and Creep Properties of Arc-Melted and Electron-Beam-Melted Tungsten at 2250° to 4140°F," *Trans. AIME*, Vol. 233, p. 1860.
- [25] Flagella, P. N., 1967, "High Temperature Creep-Rupture Behavior of Unalloyed Tungsten," *Proceedings of the Third International Symposium on High Temperature Technology*, Butterworths, p. 279.
- [26] Henshall, G. A., 1987, "Solute-Enhanced Back Stresses and Their Role in a Simplified Phenomenological Constitutive Model for the Nonelastic Deformation of Metals and Alloys," *Ph.D. Thesis*, Stanford University.
- [27] Verrilli, M. J., 1988, unpublished experimental data, NASA.
- [28] Yan, B.-D., and Laird, C., 1985, "The Phenomenon of Strain Avalanches in Cyclic Deformation," *Acta Metall.*, Vol. 33, p. 2023.
- [29] Lamba, H. S., and Sidebottom, O. M., 1978, "Cyclic Plasticity for Nonproportional Paths: Part 2 - Comparison With Predictions of Three Incremental Plasticity Models," *J. Eng. Mater. Technol.*, Vol. 100, p. 104.
- [30] Il'yushin, A. A., 1954, "On the Relations Between Stresses and Small Deformations in Mechanics of Continuous Media," *PPM J. Appl. Math. Mech.*, Vol. 18, p. 641.
- [31] Sherby, O. D., and Miller, A. K., 1979, "Combining Phenomenology and Physics in Describing the High Temperature Mechanical Behavior of Crystalline Solids," *J. Eng. Mater. Technol.*, Vol. 101, p. 387.
- [32] Walker, K. P., and Jordan, E. H., 1985, "Biaxial Constitutive Modelling and Testing of a Single Crystal Superalloy at Elevated Temperatures," presented at: *Biaxial and Multiaxial Fatigue Conference*,

Sheffield, England. Published in: *Biaxial and Multiaxial Fatigue, EGF3*, M. W. Brown and K. J. Miller, eds., Mechanical Engineering Publications, 1989, p. 145.

- [33] Marquis, D., 1979, "Modélisation et Identification de L'érouissage Anisotrope des Métaux," *Ph.D. Thesis*, Université Pierre et Marie Curie, Paris.

APPENDIX A

WALKER IMPLICIT INTEGRATION METHOD

A recursive integration relation for a linear, first-order, differential equation is given. The uniformly-valid asymptotic expansion of WALKER [6] is applied to this integral equation. In the past, this method has been applied to specific viscoplastic models retaining only the first term in the expansion [6,7]. Here we apply it to a general differential equation so that its structure is more fully revealed, and it is extended to include the second term in the expansion.

Consider the linear, first-order, differential equation

$$\dot{X} + \dot{u} X = \dot{v} \quad (A1)$$

where \dot{u} and \dot{v} are the parameters, which may be nonlinear functions of X , and X is the variable to be solved for. One can integrate this differential equation over the time interval $[0, t+\Delta t]$ and obtain

$$\begin{aligned} X(t+\Delta t) &= X_0 e^{-u(t+\Delta t)} + \int_{\xi=0}^{t+\Delta t} \exp\left[-\int_{\xi}^{t+\Delta t} \frac{\partial u(\tau)}{\partial \tau} d\tau\right] \frac{\partial v(\xi)}{\partial \xi} d\xi \\ &= X_0 e^{-u(t+\Delta t)} + \int_{\xi=0}^{t+\Delta t} e^{-[u(t+\Delta t) - u(\xi)]} \frac{\partial v(\xi)}{\partial \xi} d\xi \end{aligned} \quad (A2)$$

where $X_0 = X(0)$. The integral in this equation is the nonhomogeneous contribution to the solution of the differential equation (A1). This integral equation can be cast into a recursive relation by dividing the interval of integration into two parts, *viz.*,

$$\begin{aligned} X(t+\Delta t) &= X_0 e^{-u(t+\Delta t)} + \int_{\xi=0}^t e^{-[u(t+\Delta t) - u(\xi)]} \frac{\partial v(\xi)}{\partial \xi} d\xi + \\ &+ \int_{\xi=t}^{t+\Delta t} e^{-[u(t+\Delta t) - u(\xi)]} \frac{\partial v(\xi)}{\partial \xi} d\xi \end{aligned} \quad (A3)$$

Substituting the identity $1 = e^{-u(t)} e^{u(t)}$ into the first integral of this equation results in

$$\begin{aligned} X(t+\Delta t) &= X_0 e^{-u(t+\Delta t)} + e^{-[u(t+\Delta t) - u(t)]} \int_{\xi=0}^t e^{-[u(t) - u(\xi)]} \frac{\partial v(\xi)}{\partial \xi} d\xi + \\ &+ \int_{\xi=t}^{t+\Delta t} e^{-[u(t+\Delta t) - u(\xi)]} \frac{\partial v(\xi)}{\partial \xi} d\xi \end{aligned} \quad (A4)$$

which simplifies to the desired recursive integral equation

$$X(t+\Delta t) = X(t) e^{-[u(t+\Delta t) - u(t)]} + \int_{\xi=t}^{t+\Delta t} e^{-[u(t+\Delta t) - u(\xi)]} \frac{\partial v(\xi)}{\partial \xi} d\xi \quad (A5)$$

where $t \geq 0$ and $u(0) = X(0) = 0$. The derivation of this relation made use of eqn. (A2) when integrated over the time interval $[0, t]$.

The recursive relation given by eqn. (A5) for the differential relation in eqn. (A1) becomes practical only when a solution strategy exists for evaluating the integral

$$I(\Delta t) = \int_{\xi=t}^{t+\Delta t} e^{-[u(t+\Delta t) - u(\xi)]} \frac{\partial v(\xi)}{\partial \xi} d\xi \quad (A6)$$

When $u(t)$ is a monotonically increasing function of t , this integral possesses an evanescent memory of the forcing function $\partial v(\xi)/\partial \xi$, causing most of the contribution to the integral to come from the region near the

upper limit $\xi \approx t + \Delta t$, where the exponential term is approximately equal to its maximum value of 1. Using the method of Laplace, WALKER [6] derived a uniformly-valid asymptotic expansion for this integral equation by first expanding the arguments of the exponential and derivative into a Taylor series, and then integrating. In particular, by writing $u(\xi) = u[t + \Delta t - (t + \Delta t - \xi)]$ and expanding it by Taylor's theorem to give $u(\xi) = u(t + \Delta t) - (t + \Delta t - \xi) \frac{du(t + \Delta t)}{d(t + \Delta t)} + \dots$, the integral equation (A6) becomes

$$I(\Delta t) = \int_{\xi=t}^{t+\Delta t} e^{-[(t+\Delta t-\xi)\dot{u} - \dots]} \frac{\partial v(\xi)}{\partial \xi} d\xi \quad (\text{A7})$$

which can be rewritten in equivalent form as

$$I(\Delta t) = - \int_{z=0}^{\Delta t} e^{-z\dot{u} - \dots} \frac{\partial v(t + \Delta t - z)}{\partial z} dz \quad (\text{A8})$$

by introducing the change in variable $z = t + \Delta t - \xi$. If one now expands the argument of the derivative in this integrand using Taylor's theorem to give $v(t + \Delta t - z) = v(t + \Delta t) - z \frac{dv(t + \Delta t)}{d(t + \Delta t)} + \dots$, then this derivative can be represented by the series $\frac{\partial v(t + \Delta t - z)}{\partial z} = - \frac{\partial v(t + \Delta t - z)}{\partial(t + \Delta t)} = -\dot{v} + z\ddot{v} - \dots$, and the integral in eqn. (A8) can be expressed as

$$I(\Delta t) = \int_{z=0}^{\Delta t} e^{-z\dot{u} - \dots} (\dot{v} - z\ddot{v} + \dots) dz \quad (\text{A9})$$

Integrating this relationship gives a uniformly valid asymptotic expansion for the integral in eqn. (A6); viz.,

$$I(\Delta t) \approx \frac{\dot{v}}{\dot{u}} \left[1 - e^{-\dot{u}\Delta t} \right] + \frac{\ddot{v}}{\dot{u}} \left[\Delta t e^{-\dot{u}\Delta t} - \frac{1}{\dot{u}} \left[1 - e^{-\dot{u}\Delta t} \right] \right] \quad (\text{A10})$$

where the third and higher-order terms in the expansion have been neglected. Here we recall that the derivatives of u and v are evaluated at time $t + \Delta t$.

A uniformly-valid, implicit, numeric, integration method providing a solution strategy to the recursive integral equation (A5) for the linear, first-order, differential equation (A1) is therefore given by the difference relation

$$\begin{aligned} X(t + \Delta t) = & X(t) e^{-\Delta u(t + \Delta t)} + \frac{\Delta v(t + \Delta t)}{\Delta u(t + \Delta t)} \left[1 - e^{-\Delta u(t + \Delta t)} \right] + \\ & + \frac{\Delta v(t + \Delta t) - \Delta v(t)}{\Delta u(t + \Delta t)} \left[e^{-\Delta u(t + \Delta t)} - \frac{1}{\Delta u(t + \Delta t)} \left[1 - e^{-\Delta u(t + \Delta t)} \right] \right] \end{aligned} \quad (\text{A11})$$

where $\Delta x(t + \Delta t) \equiv x(t + \Delta t) - x(t) \approx \dot{x}(t + \Delta t)\Delta t$, $\Delta \dot{x}(t + \Delta t) \equiv \dot{x}(t + \Delta t) - \dot{x}(t) \approx \ddot{x}(t + \Delta t)\Delta t$, and hence $\Delta x(t + \Delta t) - \Delta x(t) \approx [\dot{x}(t + \Delta t) - \dot{x}(t)]\Delta t \approx \ddot{x}(t + \Delta t)(\Delta t)^2$ for a constant time step size Δt . This implicit integration scheme must be solved iteratively, since $\Delta u(t + \Delta t)$ and $\Delta v(t + \Delta t)$ may be nonlinear functions of $X(t + \Delta t)$.

The implicit integration method of eqn. (A11) is valid for an arbitrary time step size $\Delta t > 0$, be it large or small, even when only the first term in the expansion is retained, i.e., it is uniformly valid. This follows because whenever $\Delta u \gg 1$, or equivalently $\Delta u X \gg \Delta X$, eqn. (A11) reduces to

$$X(t + \Delta t) \approx \frac{\Delta v(t + \Delta t)}{\Delta u(t + \Delta t)} \quad (\text{A12})$$

and whenever $\Delta u \ll 1$, or equivalently $\Delta u X \ll \Delta X$, it reduces to

$$X(t + \Delta t) \approx X(t) + \Delta v(t + \Delta t) \approx X(t) + \Delta X(t + \Delta t) \quad (\text{A13})$$

when keeping only the first term in the asymptotic expansion, or to

$$\begin{aligned} X(t + \Delta t) & \approx X(t) + \frac{1}{2}[\Delta v(t + \Delta t) + \Delta v(t)] \\ & \approx X(t) + \frac{1}{2}[\Delta X(t + \Delta t) + \Delta X(t)] \end{aligned} \quad (\text{A14})$$

when keeping the first two terms in the asymptotic expansion, as in eqn. (A11). Equation (A12) is the asymptotic solution to eqn. (A1) whenever $\Delta u X \gg \Delta X$, and eqns. (A13 and A14) are valid whenever $\Delta u X \ll \Delta X$. In fact, eqn. (A13) is the Euler backward difference method, while eqn. (A14) is the trapezoidal difference method. Because keeping the second term of the asymptotic expansion comes with negligible computational expense per iteration (one must only retain $\Delta v(t)$ from the previous time step), and because numerical experiments show that this reduces the number of iterative steps required to attain convergence, it is therefore recommended that the second term in the asymptotic expansion be retained in numeric algorithms.

Viscoplastic models are composed of systems of stiff, linear, first-order, differential equations with coupled nonlinear parameters. An algorithm for the numeric solution of these models using the implicit integration scheme of eqn. (A11) (where only the first term in the asymptotic expansion was kept) and the iterative technique of Newton-Raphson is given in ref. 6. An earlier algorithm of WALKER's [1] (where the derivatives of u and v are evaluated at time t instead of time $t+\Delta t$) is not as efficient.

Even though this integration scheme is stable and accurate for time steps of arbitrary size from the numerical viewpoint, it will still be necessary to moderate the time step size from a physics viewpoint in order to properly trace the loading history, especially when it is nonproportional such that the principal axes of tensor-valued variables rotate in a material reference frame. The evolutionary equations in unified viscoplastic formulations introduce an evanescent strain memory effect (evanescent along the inelastic strain path). This effect is consistent with IL'YUSHIN's [30] delay-trace hypothesis, that a material's response depends not on the whole of the previous strain path, but only on the most recent part of it. This physical fact is assimilated in the integration algorithm by expanding the exponential integrand in eqn. (A6) about the current state.

APPENDIX B

MODEL DEVELOPMENT AND CHARACTERIZATION

Here we derive the material functions given in eqn. (6) that are unique to this model, and present a methodology for determining values for the material constants of the model.

MILLER'S HYPOTHESIS

The Zener parameter Z in the flow equation (3a) is a temperature normalized function describing the magnitude of inelastic strain rate, *i.e.*, $Z = |\dot{\epsilon}^p|/\theta$. At steady state, one must be able to express Z as only a function of stress, since the internal variables do not evolve at steady state. Therefore, one can propose two distinct Zener parameters, each differing in argument and function; one for steady states, and the other for transient states. If one defines these arguments as

$$Z_{ss} = Z_{ss} \left[\frac{|S|}{A} \right], \quad Z = Z \left[\frac{|S-B|}{D} \right] \quad (\text{B1})$$

then the *hypothesis of Miller* [2] given by

$$Z = Z_{ss} \left[\left[\frac{|S-B|}{D} \right]^m \right] \quad (\text{B2})$$

establishes the functional dependence of the transient Zener parameter Z (the harder of the two to characterize) in terms of the steady-state Zener parameter Z_{ss} . Here $A > 0$ is a material constant introduced to normalize the units, and $m \geq 1$ is the constant-structure exponent.

The advantages of this hypothesis go beyond just providing the functional form for the transient Zener parameter. One can now equate arguments between the Z of eqn. (B2) and the Z_{ss} of eqn. (B1) under steady state conditions. Assuming that the steady-state value for back stress is proportional to the value of applied stress, *i.e.*,

$$|B|_{ss} = b |S| \quad (\text{B3})$$

then it immediately follows that

$$D_{ss} = A(1-b) \left(\frac{|S|}{A} \right)^{\frac{m-1}{m}} \quad (\text{B4})$$

independent of the choice of functional form for Z_{ss} . Actually, Miller proposed eqn. (B4) and then derived eqn. (B3), where the proposition of eqn. (B4) was based on data from warm-worked material. These relationships play an important role in characterizing the thermal recovery functions. Note that $m = 1$ implies $D_{ss} = A(1-b) = \text{constant}$, but in the model of eqn. (6) $m > 1$ because of the recovery function r .

MATERIAL FUNCTIONS

A steady-state Zener parameter that is the sum of two power-law functions, *i.e.*,

$$Z_{ss} = \left[\frac{|S|}{A} \right]^n + \left[\frac{A}{A'} \right]^{n'} \left[\frac{|S|}{A} \right]^{n'} \quad (\text{B5})$$

is proposed, and we motivate this choice with the steady-state creep data of fig. 1. Applying Miller's hypothesis, eqn. (B2), to this form for Z_{ss} results in the transient Zener parameter Z given in eqn. (6b). The function for thermal diffusivity, eqn. (6a), was derived by MILLER [2].

The limit function L for the short-range back stress controls the degree of curvature exhibited at the knee of the stress-strain curve. Equation (6c) assumes that L is proportional to the value of the drag strength. This relationship is in accordance with the physical observation that a material's capacity to sustain an internal stress (of which L is the measure) is directly related to the density and distribution of its dislocation substructures (of which D is the measure).

By definition $\dot{B}_{ij} = 0$ at steady state, and therefore from the constitutive equation (2b) one obtains

$$\dot{B}_{ij} = \frac{2}{3} \left[H_1 \dot{\beta}_{ij}^1 + H_2 \dot{\beta}_{ij}^2 \right] = 0 \quad (\text{B6})$$

from which one derives the thermal recovery function R for the back stress. Here it is considered that $\dot{T} = 0$ at steady state, which implies that $\dot{H}_1 = \dot{H}_2 = 0$ at steady state. Combining this relationship with the evolution equations (3) for β_{ij}^1 and β_{ij}^2 , and using the fact that X_{ij} , B_{ij}^2 , and S_{ij} are coaxial with each other at steady state (a direct consequence of the chosen evolution equations), leads to

$$R = \left[\frac{H_1 + H_2}{H_1} - \frac{|X|}{L} \right] Z_{ss} \quad (\text{B7})$$

which when combined with eqns. (B3 and B5) results in the expression for the thermal recovery function R given in eqn. (6d).

At steady state, $\dot{D} = 0$ by definition, and therefore the evolution equation (3d) for drag strength reduces to

$$\theta r = \frac{D}{D - D_0} \frac{|S - B|}{D} \Big|_{ss} \dot{\epsilon}^p = \theta \frac{D}{D - D_0} \left[\frac{|S|}{A} \right]^{\frac{1}{m}} Z_{ss} \quad (\text{B8})$$

where eqns. (B3 and B4) are used to reduce the coefficient $|S - B|/D$ in the middle expression. Combining eqns. (B4, B5, and B8) results in the thermal recovery function r for drag strength presented in eqn. (6f).

MATERIAL CONSTANTS

For a complete material description using the model presented herein, there are: three elastic constants: E , α , and ν ; two thermal constants: Q and T_i ; four steady state constants: A , A' , n , and n' ; the constant-structure constant: m ; two threshold constants: b and c ; three transient constants: h , H_1 , and H_2 ; the nonproportionality constant: a ; and the initial value: D_0 . Their values are given in table 1 for aluminum, copper, nickel, and tungsten. There are seventeen independent material constants in all, which to a good approximation are temperature insensitive. There are a number of *rules of thumb* (or estimates) given below that one can use to assign values to the various constants if data are unavailable.

The activation energy for self diffusion $Q > 0$ and the melting temperature $T_m > 0$ are typical handbook data. A useful estimate is that the transition temperature $T_i > 0$ associated with the activation energy for inelastic flow is given by $T_i \approx 0.6T_m$ with actual values ranging between $0.5T_m$ and $0.8T_m$ [31].

With the thermal diffusivity now characterized, one can determine the steady-state Zener parameter $Z_{ss} = |\dot{\epsilon}^p|_{ss}/\theta$ from creep data and plot it against its associated flow stress, as done in fig. 1. The lines in this figure represent the fit of eqn. (B5) to the data. Values for the constants $A > 0$, $A' > 0$, $n > 0$, and $n' > 0$ are readily obtained by eye, or by the method of least squares. Since creep data are probably the most abundant of all high-temperature experimental data, one should have no difficulty in characterizing the Norton creep constants A and n ($n \approx 5$, typically). High-stress creep data, however, are sometimes scarce or unavailable. If this is the case, one can use the estimates given by: $n' \approx 3.5n$ and $Z_{co} = (A'/A)^{nn'/(n'-n)} \approx 10^{10} s^{-1}$, with values ranging between $3n$ to $4n$ for n' and 10^9 to $10^{12} s^{-1}$ for the Zener parameter Z_{co} at cross over (cf. fig. 1).

The remaining steady state constant, the Bauschinger coefficient $b \in (0,1)$ defined in eqn. (B3), can be obtained from a tensile test where a specimen is loaded to its saturation (or steady state) strength σ_{sat} , and then unloaded sufficient enough to induce some reversed plasticity. One then obtains a value for the Bauschinger coefficient from the relationship $b \approx (\sigma_{sat} + \sigma_{ry})/2\sigma_{sat}$, where σ_{ry} is the reversed yield strength. A word of caution. A small offset strain should be used to establish σ_{ry} to ensure a realistic value for b . Values for b may range from 0.2 to 0.7, with a typical value being 0.4. The larger the value for b , the greater the predicted Bauschinger effect.

There is one more material constant that one can ascertain from creep testing. It is the constant structure exponent $m > 1$ which can be determined from stress-drop tests. Fortunately, this parameter is nearly insensitive to material selection. Typical values for the constant structure exponent are: $m \approx 1.8$ for pure metals, and $m \approx 1.5$ for alloys [13].

The next step is to obtain those constants one can from stable stress-strain hysteresis loops, where the isotropic variable has saturated. Ratios of plastic strain range to elastic strain range of 1:1 to 3:1 generally work well. The constant $H_2 > 0$ represents the tangent modulus in the region of linear strain hardening after going around the knee of the curve, with $H_2 \approx H_1/100$ serving as a rule of thumb. The constant $H_1 > 0$ defines the tangent modulus at the onset of inelastic deformation. Our experience from optimization calculations is that $H_1 \approx E/5$ provides a good estimate for its value. The larger the value for the material constant c , the more rounded the knee in the hysteresis loop will be. The method of nonlinear least squares [32] is a useful tool, but not a necessary one, for determining c and H_1 (and D_{sat} since the drag strength is an unknown constant at this time) since there are three constants to be determined simultaneously at this step of material characterization.

The constants $D_0 > 0$ and $h > 0$ are characterized next. The constant h establishes the rate of isotropic hardening in monotonic tension to large strains. The initial value D_0 for drag strength is obtained by comparing predicted and experimental values for the yield strength. Some iteration between these two constants may be necessary to obtain a proper fit. Again, the method of nonlinear least squares may be helpful, but it is certainly not necessary.

The final material constant to quantify is the nonproportionality parameter $a \in [0,1]$. This requires nonproportional experimental data. If they do not exist, which is likely to be the case, setting $a = 0$ implies that the theory resembles a two-surface plasticity model with Mroz hardening [33]. Further experimental study is required before typical values for a can be given.

TABLE 1

Elastic Constants‡					
Constant	Units	Material			
		Al	Cu	Ni	W
E_0	GPa	71	127	210	395
E_1	MPa/°C	-36	-41	-2.5	-2.3
E_2	MPa/°C ²	-.011	-.027	-.063	-.027
ν	-	.34	.34	.31	.28
α_0	1/°C	25×10^{-6}	16×10^{-6}	13×10^{-6}	4.4×10^{-6}
α_1	1/°C ²	-	5×10^{-9}	-	$.16 \times 10^{-9}$
‡	$E = E_0 + E_1T + E_2T^2$ $\alpha = \alpha_0 + \alpha_1T$ T is in degrees centigrade.				
Inelastic Constants*					
Constant	Units	Material			
		Al	Cu	Ni	W
A	MPa	.076	1.2	.55	.29
A'	MPa	4.4	18	19	26
b	-	.6	.35	.5	.4†
c	-	23	7	15	10†
D_0	MPa	.1	1.2	.5	.3†
h	MPa	.05	3	2	5†
H_1	GPa	10	20	70	100†
H_2	MPa	100	200	700	1000†
m^\dagger	-	1.8	1.8	1.8	1.8
n	-	4	5.5	5	4.5
n'	-	14	19	15	19
Q	kJ/mole	140	200	290	590
T_i	°K	560	820	1000†	2600
*	Data are not available to characterize the material constant <i>a</i> , nor is there adequate experience to assign values <i>via</i> a rule of thumb.				
†	Determined by engineering judgment because of a lack of data.				

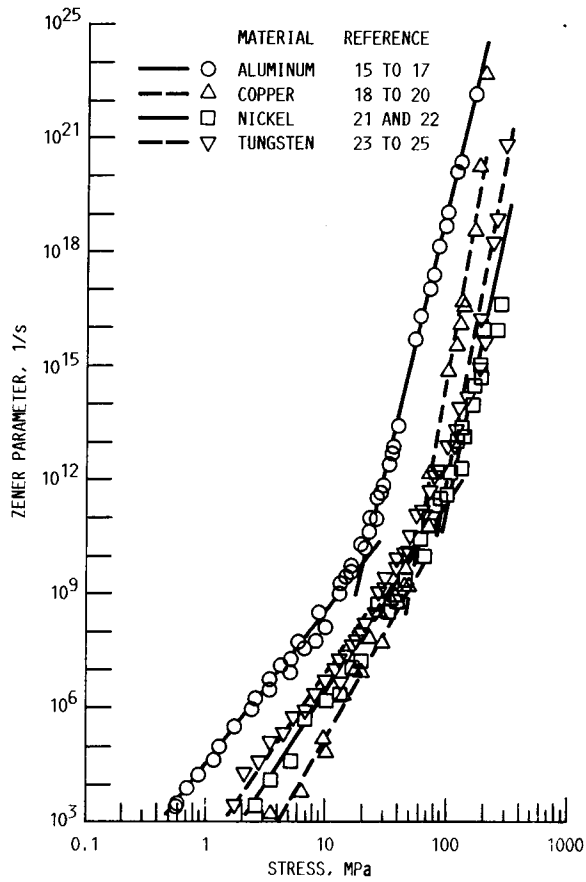


FIGURE 1. - STRESS DEPENDENCE OF ZENER PARAMETER FOR ALUMINUM, COPPER, NICKEL, AND TUNGSTEN.

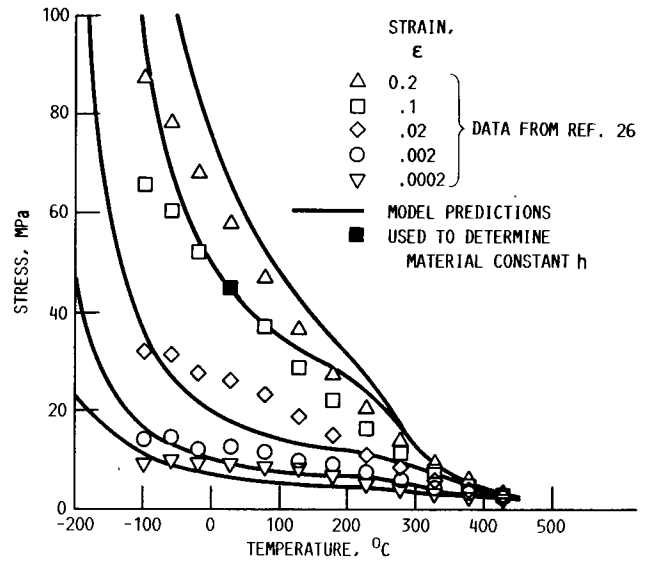


FIGURE 2. - MONOTONIC STRESS-STRAIN RESPONSE OF ALUMINUM AS A FUNCTION OF TEMPERATURE. STRAIN RATE, $\dot{\epsilon}$, 0.000128/s.

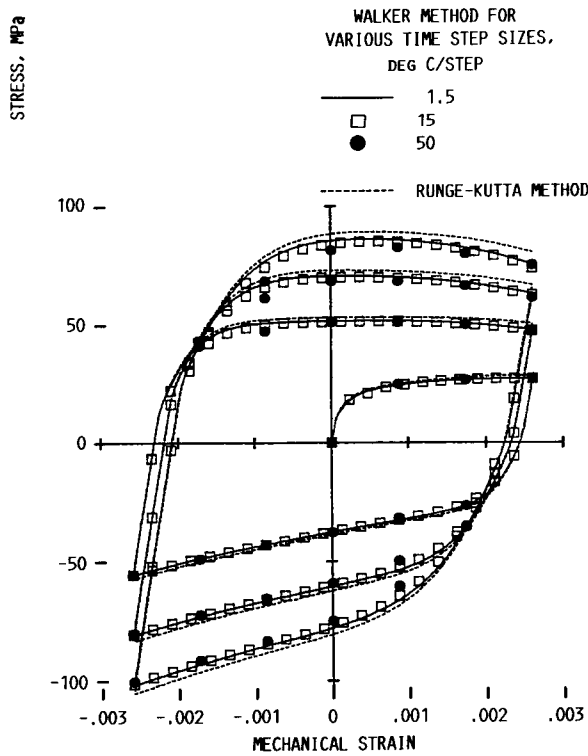
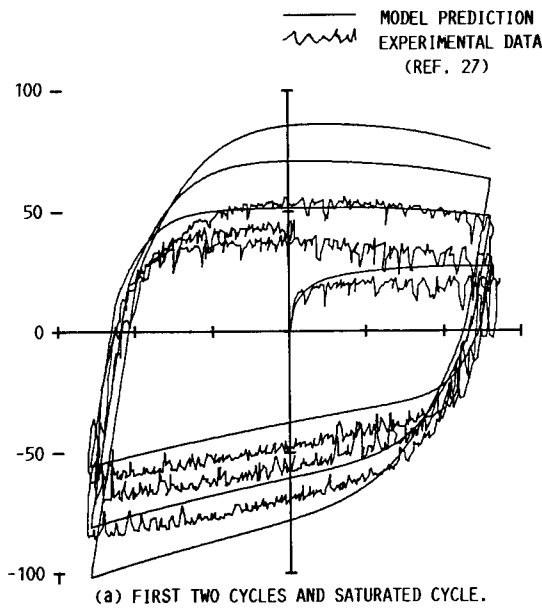


FIGURE 3. - INPHASE THERMOMECHANICAL RESPONSE OF NICKEL. CONTROL IS VIA LINEAR RAMPS IN TEMPERATURE AND MECHANICAL STRAIN WITH A 600s CYCLE TIME. TEMPERATURE RANGE, 400 TO 700 °C. MECHANICAL STRAIN RANGE, ± 0.0026 .

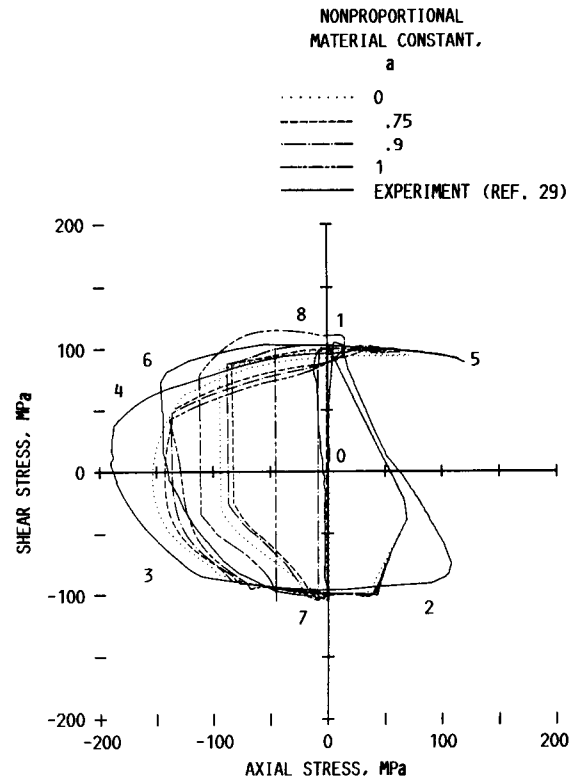
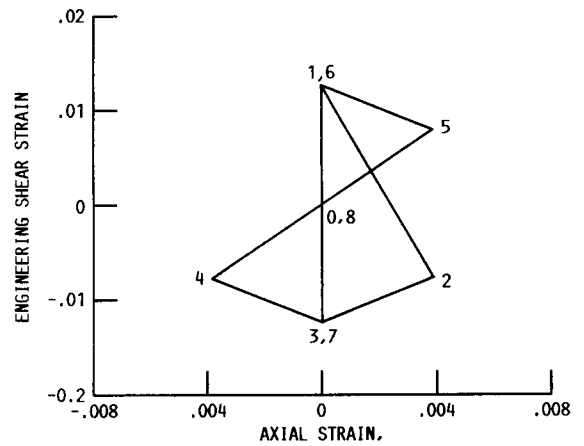


FIGURE 4. - CYCLIC, NONPROPORTIONAL, AXIAL-TORSIONAL TEST OF COPPER AT ROOM TEMPERATURE. THE TEST SPECIMEN WAS CYCLED TO ISOTROPIC SATURATION PRIOR TO TESTING.



Report Documentation Page

1. Report No. NASA TM-102338	2. Government Accession No.	3. Recipient's Catalog No.	
4. Title and Subtitle Refinements in a Viscoplastic Model		5. Report Date	
		6. Performing Organization Code	
7. Author(s) A.D. Freed and K.P. Walker		8. Performing Organization Report No. E-4988	
		10. Work Unit No. 505-63-1B	
9. Performing Organization Name and Address National Aeronautics and Space Administration Lewis Research Center Cleveland, Ohio 44135-3191		11. Contract or Grant No.	
		13. Type of Report and Period Covered Technical Memorandum	
12. Sponsoring Agency Name and Address National Aeronautics and Space Administration Washington, D.C. 20546-0001		14. Sponsoring Agency Code	
		15. Supplementary Notes Prepared for the 1989 Winter Annual Meeting of the American Society of Mechanical Engineers, San Francisco, California, December 10-15, 1989.	
16. Abstract A thermodynamically admissible theory of viscoplasticity with two internal variables (a back stress and a drag strength) is presented. Six material functions characterize a specific viscoplastic model. In the pursuit of compromise between accuracy and simplicity, a model is developed that is a hybrid of two existing viscoplastic models. A limited number of applications of the model to Al, Cu, and Ni are presented. A novel implicit integration method is also discussed, and applications are made to obtain solutions using this viscoplastic model.			
17. Key Words (Suggested by Author(s)) Viscoplasticity; Copper; Nickel; Aluminum; Tungsten		18. Distribution Statement Unclassified - Unlimited Subject Category 39	
19. Security Classif. (of this report) Unclassified	20. Security Classif. (of this page) Unclassified	21. No of pages 18	22. Price* A03